Electric and Magnetic Properties of Atomic Layer Deposited ZrO_2-HfO_2 Thin Films

Kristjan Kalam,[1,z] Helina Seemen,[1] Mats Mikkor,[1] Peeter Ritslaid,[1] Raivo Stern,[2] Salvador Dueñas,[3] Helena Castán,[3] Aile Tamm,[1] and Kaupo Kukli[1,4]

[1]*Institute of Physics, University of Tartu, 50411 Tartu, Estonia*
[2]*National Institute of Chemical Physics and Biophysics, 12618 Tallinn, Estonia*
[3]*Department of Electronics, University of Valladolid, 47011 Valladolid, Spain*
[4]*Department of Chemistry, University of Helsinki, FI-00014 Helsinki, Finland*

Atomic layer deposition method was employed to deposit thin films consisting of ZrO_2 and HfO_2. Zirconia films were doped with hafnia and vice versa, and also nanolaminates were formed. All depositions were carried out at 300°C. Most films were crystalline in their as-deposited state. Zirconia exhibited the metastable cubic and tetragonal phases by a large majority, whereas hafnia was mostly in its stable monoclinic phase. Magnetic and electrical properties of the films were assessed. Un-doped zirconia was ferromagnetic and this property diminished with increasing the amount of hafnia in a film. All films exhibited ferroelectric-like behavior and the polarization curves also changed with respect to the film composition.
 [DOI: 10.1149/2.0041809jss]

Manuscript submitted May 22, 2018; revised manuscript received July 29, 2018. Published August 9, 2018.

HfO_2 and ZrO_2 thin films have many applications, for example HfO_2 films are used as heat mirrors for energy-efficient windows,[1] both ZrO_2 and HfO_2 can serve as optical coatings,[2–4] waveguides,[5–7] gas sensors,[8–10] gate dielectrics in transistors.[11–13] Proposed applications also include novel memory materials, such as resistive switching memory elements[14–17] and ferroelectric memories.[18–20]

ZrO_2 and HfO_2 have also been recognized as potential magnetic materials, mostly when doped with some other material, for example Mn-doped zirconia,[21] Fe, Co and Ni doped zirconia,[22] Sc, Ti, Ta, Fe and Co doped hafnia.[23]

HfO_2 and ZrO_2 thin films have been prepared via reactive sputtering,[24,25] pulsed laser deposition,[2,26] electron beam evaporation,[27,28] chemical vapor deposition[29,30] and spray pyrolysis.[31,32]

HfO_2 thin films have been atomic layer deposited (ALD) from hafnium tetrakis(dimethylamide) and water on Si(100) substrates in the temperature range of 205–400°C.[33] Hafnium tetrakis(ethylmethylamide) and water were used as precursors for depositing the films on Si(100),[34] TiN[19] or Ni, Pt and Pd.[35] Atomic layer deposited hafnia has been made from $HfCl_4$ and H_2O at 300°C.[36,37] Film growth at 300°C was analyzed for comparison, using different metal precursors $HfCl_4$ and HfI_4, and the oxidizer was water.[38] $HfCl_4$-H_2O and HfI_4-O_2 processes were compared in the temperature range of 300–600°C.[39] HfO_2 and ZrO_2 have been fabricated, using $Hf[N(CH_3)_2]_4$ (TDMA-HF) and ZyALD ((tris(dimethylamino)cylcopentadienyl)-zirconium), as respective Hf and Zr precursors, and O_3 as oxidizer, at 260°C and 285°C.[20] ZrO_2 films have been atomic layer deposited using $(CpMe)_2ZrMe_2$ and $(CpMe)_2Zr(OMe)Me$ as Zr precursors, and O_3 as the oxidant at 300 or 350°C.[40] ZrO_2 films from tris(dimethylamino)cyclopentadienylzirconium $CpZr(NMe_2)_3$ and H_2O, were investigated using real-time characterization of the growth process at substrate temperatures ranging from 120 to 350°C.[41] ZrO_2 growth has been carried out in the case of $ZrCl_4$ and H_2O as precursors[37] and this process has also been monitored in real time.[42] Zirconia has also been deposited from TEMAZ (tetrakis(ethylmethylamide) zirconium) and water.[19,35]

Atomic layer deposited HfO_2 and ZrO_2 nanolaminates[20] and mixtures[19] were investigated and found to be ferroelectric. Microstructural evolution of ALD-grown HfO_2-ZrO_2 nanolaminates was studied.[37] Atomic layer deposited $Hf_{0.5}Zr_{0.5}O_2$ films have also shown to be ferroelectric.[35]

This study is devoted to ALD of mixed or laminated thin films consisting of ZrO_2 and HfO_2. The purpose was to evaluate the structure and composition of the deposited films and how they influence the magnetic and electrical properties, more specifically, the materials ability to polarize in magnetic and electric fields. The hypothesis was that films consisting of ZrO_2 and HfO_2 should exhibit both ferroelectric and ferromagnetic properties and the goal was to find out the structure and composition, for which both of these properties appear in the same material.

Experimental

The films studied in this work were grown in a low-pressure flow-type ALD reactor.[43] $HfCl_4$, 99,9%, supplied by Alfa Aesar, was used as the hafnium precursor and was evaporated at 162°C. Zirconium precursor, 99,9% $ZrCl_4$, supplied by Aldrich, was evaporated at 160°C. Both metal precursors were evaporated from a glass boat inside the reactor. Nitrogen, N_2 (99.999% purity, Eesti AGA AS), was applied as the carrier and purging gas. Water was used as an oxidizer and the ALD reactions were carried out at 300°C.

Films were deposited by alternating metal and oxygen precursors in sequential ALD cycles with certain cycle ratios. For example, hafnia was doped with zirconia in the following manner: 10 ALD cycles of HfO_2 was deposited, onto which 1 ALD cycle of ZrO_2 was deposited and this sequence was repeated 9 times. Total amount of cycles was kept at about a 100 for each deposition. Cycle ratios of HfO_2 and ZrO_2 were varied as such: 10:1, 10:3, 10:5, 10:10, 5:10, 3:10, 1:10, 2:1. Also, two nanolaminates were prepared: 50 cycles of hafnia + 50 cycles of zirconia and vice versa. The cycle times for ZrO_2 were 4-4-2-8 s for the sequence $ZrCl_4$ pulse – N_2 purge – O_3 pulse – N_2 purge. Cycle times for an analogous HfO_2 growth cycle were 4-3-2-7 s.

Films were grown on Si(100) cleansed and etched[44] and highly-doped conductive Si substrates covered by 10 nm thick TiN film grown by chemical vapor deposition. The films, which were deposited on TiN substrates for electrical measurements, were also supplied with Ti/Al electrodes (area 0.204 mm^2) electron-beam evaporated on top of the films, with ca. 30 nm thick Ti layer in direct contact to the films. The structure to conduct electrical measurements was, from top to bottom, Al/Ti/Functional layer/TiN/Si/Al.

Spectroscopic ellipsometer (SE), model GES5-E, was used for the measurements of the films thicknesses and refractive indexes. Ellipsometric data was modelled in the range of 1.3–4.5 eV using the Cauchy dispersion model. X-ray fluorescence (XRF) spectrometer Rigaku ZSX 400 and program ZSX Version 5.55 was used to measure the elemental composition of films. The crystal structure was evaluated by grazing incidence X-ray diffractometry (GIXRD), using a X-ray diffractometer SmartLab Rigaku with CuKα radiation,

[z]E-mail: kristjan.kalam@ut.ee

Table I. Thicknesses and cation ratios of samples deposited with variable HfO_2:ZrO_2 ALD cycle ratio. Two HfO_2+ZrO_2 double layers were also deposited, with 50 ALD cycles of one constituent oxide followed by 50 cycles for another oxide.

Cycle ratio	Thickness, nm	Hafnia content Hf/(Zr+Hf)
HfO_2 reference film	24	1
ZrO_2 reference film	35	0
HfO_2:ZrO_2 1:10	17	0.17
HfO_2:ZrO_2 3:10	10	0.46
HfO_2:ZrO_2 5:10	14	0.64
HfO_2:ZrO_2 10:10	20	0.47
HfO_2:ZrO_2 10:5	18	0.91
HfO_2:ZrO_2 10:3	14	0.73
HfO_2:ZrO_2 10:1	22	0.90
HfO_2:ZrO_2 2:1	12	0.48
HfO_2+ZrO_2 50 + 50	18	0.55
ZrO_2+HfO_2 50 + 50	14	0.42

which corresponds to an X-ray wavelength of 0.15406 nm. Surface morphology of films was evaluated by scanning electron microscopy (SEM) using a Dual Beam equipment FEI Helios NanoLab 600.

Electrical polarization measurements were performed by means of an Agilent DXO-X 3104 digital oscilloscope with a built-in wave generator. The standard Sawyer-Tower experiment was carried out by applying a periodic triangular-shaped stimulus and recording the voltage loops data from the oscilloscope. Charge values were obtained from the sensed voltage across a stated capacitance.

Magnetic measurements were performed using Vibrating Sample Magnetometer (VSM) option of the Physical Property Measurement System 14T Quantum Design by scanning the magnetic field from −1 to 1 T parallel to the film surface at room temperature.

Results and Discussion

Film growth and composition.—Total amount of ALD cycles was kept near one hundred for each deposition to obtain comparable thicknesses of films, except for un-doped reference films. Thicknesses, however, varied quite substantially – from 10 to 22 nm (Table I). These results allowed one to believe that for various cycle ratios the growth rates are quite different. The lowest thicknesses were measured for the cycle ratio of 10:3, regardless of which oxide was deposited in majority (Table I). This is probably due to three ALD cycles not being enough to complete the growth of a continuous layer, but also inhibiting the growth of other oxide more than one ALD cycle does.

Hafnia doped with zirconia systematically exhibited larger thickness values for the same cycle ratios and cycle amounts than zirconia doped with hafnia. This was in spite of un-doped zirconia exhibiting higher growth rate than un-doped hafnia in the case of 200 ALD cycles. Examining the experimental Hf/(Hf+Zr) ratios, it appears that in the very beginning of growth, i.e. during the first 10 cycles, hafnia grows faster than zirconia.

Investigating the nanolaminates, it seems that, during the first 50 cycles, zirconia grows equally well on Si(100) substrate and hafnia, but hafnia grows faster on Si(100) than on zirconia.

Film structure.—All the samples were investigated in their as-deposited state. Hafnia was, by a vast majority, in its stable monoclinic form (PDF Card 01-075-4290). A low amount of cubic hafnia (PDF Card 00-053-0560) was also present (Fig. 1). Zirconia, on the other hand, was cubic or tetragonal – the width and intensities of the reflections in the patterns obtained and presented in this work did not allow one to clearly distinguish between the two lattice types (PDF Card 01-077-3168). A low amount of monoclinic zirconia (PDF Card 01-075-6446) was also distinguishable in the un-doped zirconia. Doping has evidently stabilized the metastable phase and monoclinic phase did not appear. Also, in un-doped zirconia, a peak attributable to the 103 reflection of orthorhombic ZrO_2 appeared at 56° (Fig. 1). (PDF

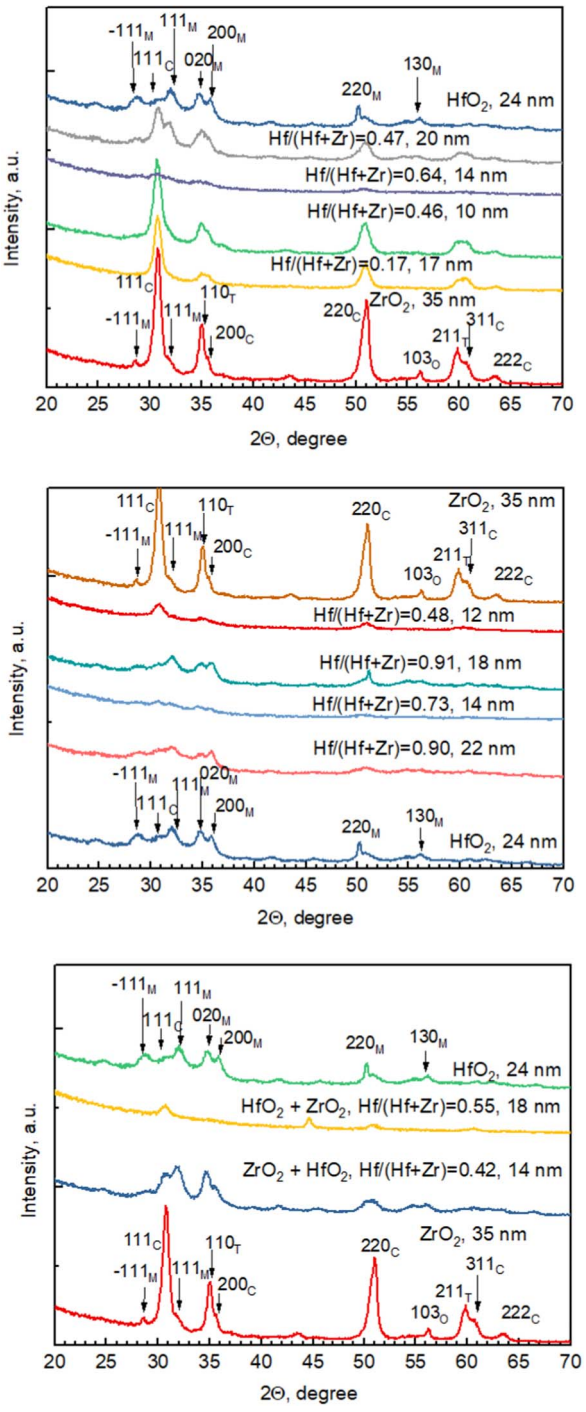

Figure 1. GIXRD patterns for un-doped ZrO_2, HfO_2 and hafnia-doped zirconia in the top panel. Zirconia-doped hafnia with reference films in the middle panel and nanolaminates with reference films in the bottom panel. The composition and thicknesses of the films are indicated by the labels at the patterns. Miller indexes are attributed to corresponding monoclinic (M), cubic (C), tetragonal (T) and orthorhombic (O) phases.

Card 00-034-1084). Films, which consisted of both metal oxides, exhibited the same GIXRD peaks as both un-doped zirconia and hafnia reference films, but the peaks in the mixed and laminated films were less intense. This can be due to the lower thicknesses of the doped films and nanolaminates, but also the degree of crystallinity is lower in such films, because mixing the oxides makes it more difficult for either single oxide to crystallize. Some patterns of mixed films had almost no distinguishable GIXRD peaks at all.

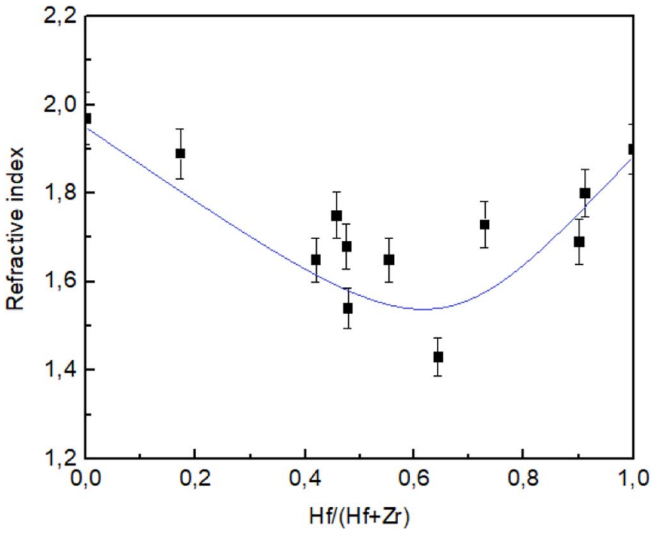

Figure 2. Refractive index at 633 nm against relative hafnia content. Solid line is a guide to eye.

Refractive index of un-doped zirconia and hafnia were found to be 1.97 and 1.90 (at 633 nm), respectively. These values are slightly lower than values commonly presented in literature. For example, HfO_2, grown by ALD at 300°C by Aarik et al.,[45] has possessed refractive index of 2.00. Aarik et al.[46] have also measured ALD-grown ZrO_2 with refractive index of 2.20. All doped films had even lower refractive indexes, most likely due to the lower density of the films (Fig. 2). The two films with recognizably low refractive indexes (below 1.6) both had significantly lower densities than other films (about 35% porosity). The lowest refractive index was measured in the case of about 60% Hf in the total amount of cations. Scattered data in the graph, i.e. different refractive indexes for the films with quite similar composition, could be explained with fluctuations in crystallinity – samples with refractive indexes higher than the overall trend are probably more strongly crystallized. Small fluctuations in composition, i.e. relative content of constituent metals, as well as deposition parameters, may induce fluctuations in phase composition, crystal growth and electron density. These fluctuations may become complicated to conveniently determine by X-ray diffraction studies, but they may induce notable changes in optical density of the solid layer.

It is noteworthy, that despite marked scatter in refractive index values, one may recognize an implication of dependence between refractive index and composition (Fig. 2). It is likely, that the films with dominating content of either HfO_2 or ZrO_2 were grown relatively dense and in these films the effective refractive index tended to be higher. On the other hand, the films in which the amounts of HfO_2 and ZrO_2 were comparable, i.e. the most strongly mixed films such as those with Hf/(Hf+Zr) = 0.5..0.6, were grown as the least dense ones with the most distorted lattices as also implied by the GIXRD results. Therefore, in the films with comparable Hf and Zr contents the refractive index had to become slightly lower, as confirmed by the measurements (Fig. 2).

SEM images of HfO_2 and films which consist mostly of HfO_2 indicate that regions with larger grains alternate with smaller grains (Fig. 3). Since the substrate was Si(100) and there is no reason to assume a heterogeneous distribution of nucleation centers, it can be supposed that the deposition parameters used in these experiments favored the growth of larger grains, but they could not form yet due to the limited time for the nucleation process. As the composition of the films changed toward higher amounts of Zr, the grain sizes became more even.

Electrical and magnetic properties.—Polarization charge in the films exhibited weak tendency to saturate upon increasing the electric field strength (Fig. 4). This effect can possibly be attributed to ferroelectric behavior, but it is evident that interfacial polarization markedly contributes to the charge polarized due to leakage current through the films. Correlation between the polarization values in such loops and values of leakage current has been shown previously.[44] Electric field values, at which similar polarization charges could be recorded, increased with higher hafnia content (Fig. 4). This is possibly due to hafnia being in the stable monoclinic form. Hafnia can be regarded

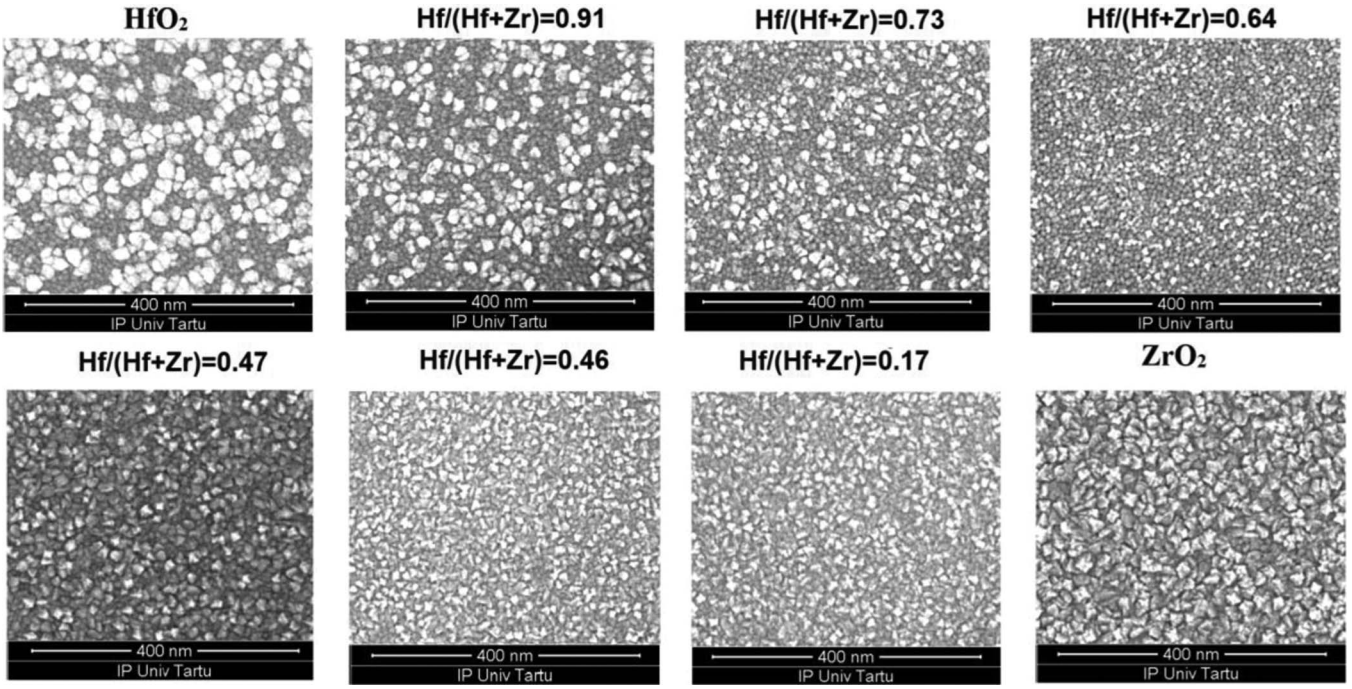

Figure 3. Scanning electron microscope images of reference hafnia, rerefence zirconia and various samples containing both oxides. Hafnia content Hf/(Hf+Zr) for each sample is denoted above each panel.

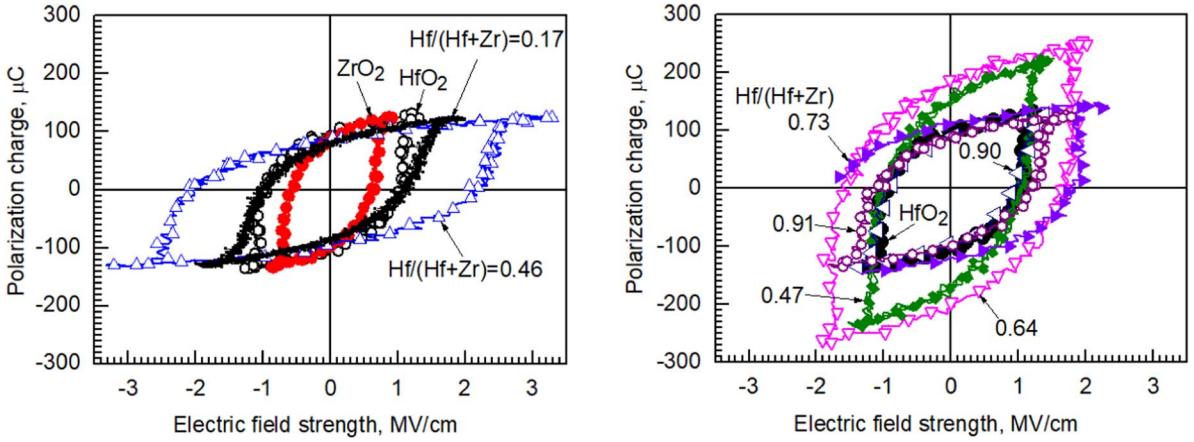

Figure 4. Polarization charge versus applied electric field curves. The left panel depicts films which are mostly in the cubic or tetragonal phase of zirconia, monoclinic hafnia is given for comparison. Right panel has curves for films which major lattice type is the monoclinic hafnia. The composition of the metal oxide layers are indicated by labels.

as more stable and less defective than zirconia, hence the preference to form a monoclinic phase. A less defective material also exhibits lower leakage, which probably accounts for the lowering of charge polarization values with the increasing content of hafnia.

The same possible reasons, why hafnia exhibits lower values for charge polarization, may explain, why it does not show ferromagnetic properties. The chemically more stable hafnia is less defective, has less oxygen vacancies and therefore does not magnetize as well as zirconia, which is ferromagnetic. Figure 5 shows hafnia having the lowest magnetization values and the magnetization increasing with the zirconia content. Un-doped zirconia film still did not exhibit as high magnetization as the nanolaminate consisting of 10 nm thick hafnia and 8 nm thick zirconia, which had a saturation magnetization of $5 \cdot 10^{-6}$ emu and a coercivity of 50 Oe. Figure 6 illustrates the magnetic and electric properties of the aforementioned nanolaminate and the inset on the left panel of Figure 6 is an enlargement of the scale near the origin of the graph to indicate coercivity values. One can see, that ferromagnetic properties can be observed in a material which also demonstrates electronic charge-voltage loops with some contribution from ferroelectric-like polarization.

In regard and to compare with literature data, Böscke et al.[18] have grown HfO_2 thin films doped with silicon (oxide) by ALD using tetrakis(ethylmethylamino)hafnium, $Hf[N(C_2H_5)CH_3]_4$, and tetrakis(dimethylamino)silane, $Si[N(CH_3)_2]_4$, with ozone as precursors between TiN electrodes. The 8.5 nm thick films were crystallized after annealing at 1000°C. The films containing less than 4 at.% silicon consisted of a mixture of tetragonal and orthorhombic phases of HfO_2 and demonstrated optimized ferroelectric performance with remnant polarization above 10 μC/cm^2 and coercive field of 1 MV/cm.

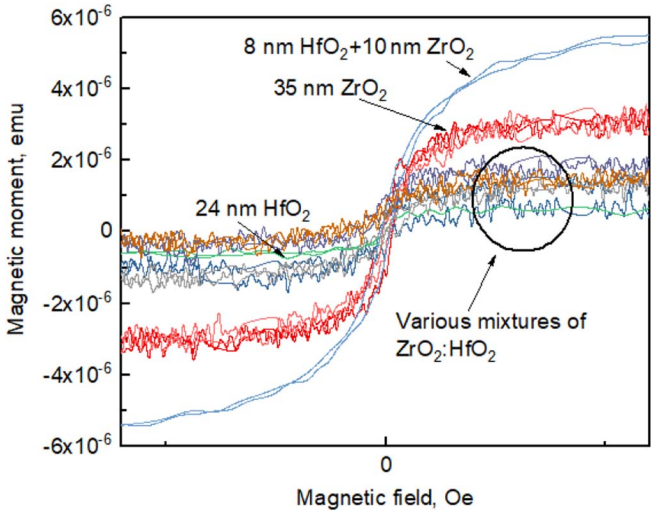

Figure 5. Magnetization versus applied magnetic field curves measured at room temperature for metal oxides described in Table I.

Müller et al.[19] deposited HfO_2 and ZrO_2 mixture films to the thickness of 9 nm, varying the pulsing ratio for $Hf[N(C_2H_5)CH_3]_4$ and $Zr[N(C_2H_5)CH_3]_4$ precursors. These films were crystallized upon TiN top electrode deposition at 500°C. Müller et al.[19] studied the effects of Zr:Hf ratio as well as the measurement temperature on the film structure and ferroelectric behavior. They observed that decrement in the relative content of Zr was followed by gradual transition between tetragonal, orthorhombic and monoclinic phases. They also observed that the application of TiN electrode tended to promote the tetragonal to orthorhombic crystallization pathway instead of that of tetragonal to monoclinic. They have measured the polarization charge hysteresis widths of approximately 2 MV, and, at nearly equal amounts of Zr and Hf, reached remanent polarization value 17 μC/cm^2, but noticed also that, due to the increasing leakage currents, the electrical measurements had to be limited to 400 K.

Lin et al.[35] have also targeted $Zr_{0.5}Hf_{0.5}O_2$ films, containing equal amounts of Zr and Hf, grown by ALD from $Hf[N(C_2H_5)CH_3]_4$ and $Zr[N(C_2H_5)CH_3]_4$ precursors. Annealing at 500–550°C was necessary to crystallize the structure. Electrical measurements revealed coercivity values even exceeding 1 MV and remanent polarization charge 19 μC/cm^2. Annealing series was provided up to 750 C. Lin et al.[35] observed that, although the contribution from orthorhombic phase seemed to increase with temperature, the heat-treatment at 750°C destroyed the ferroelectric-like polarization, likely due to the development of leakage pathways along grain boundaries.

A study by Weeks et al.[20] was devoted to ALD of HfO_2-ZrO_2 films from tetrakis(dimethylamino)hafnium, $Hf[N(CH_3)_2]_4$; tris(dimethylamino)cyclopentadienylzirconium, $CpZr(NMe_2)$ (Cp = C_5H_5, Me = CH_3); and ozone as precursors. Within the study, 8 nm thick mixtures as well as nanolaminates were fabricated, constituting of 1–4 nm thick ZrO_2 and HfO_2 layers of equal thicknesses. The as-deposited stacks had again to be annealed at 500°C for 10 min to promote crystallization. The main phase stabilized was either tetragonal or orthorhombic decided on the basis of either tetragonal 011 or orthorhombic 111 reflection detectable at 30.5 deg in XRD patterns. The hysteresis width in charge polarization loops was ca. 2 MV and the remanent polarization, as reported, was in the range of 20–39 μC/cm^2.

It is to be noted, that magnetic properties of ferroelectric hafnium zirconium oxides have not been measured in the works referred to above. In terms of structural and electrical characteristics, however,

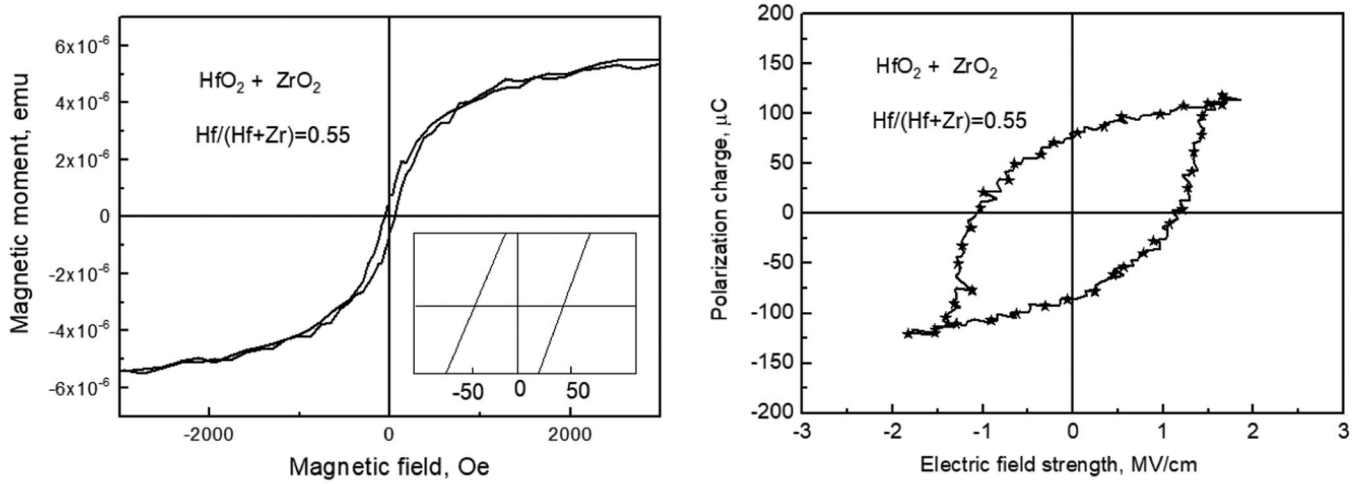

Figure 6. Magnetization-field (left panel) and electrical polarization-field (right panel) loops measured from nanolaminate film consisting of 10 nm thick HfO_2 and 8 nm thick ZrO_2 layers. Inset on the left panel is an enlargement of the origin of coordinates.

the results described in our study are to certain extent analogous to those obtained earlier. In the present study, the films were crystallized and measured in as-deposited state, since the layers were purposefully grown using chalcogenide precursors. As a common feature, the crystalline structure may not defined as unambiguously that belonging to any particular polymorph of either zirconia or hafnia, but a mixture of tetragonal and orthorhombic phases is quite likely. The width of charge polarization hysteresis tends to be quite similar to those recorded elsewhere, so the coercivity as defined, may reach 1 MV/cm. On the other hand, the polarization charge at zero external field is considerably higher than that reported earlier, up to tens of mC/cm^2. One can thus consider marked role for leaking charge interfering the polarization mechanisms. Further modifications of the structure and improvements in the performance of functional layers after, e.g., optimization of annealing parameters and/or electrode materials would form possible matter for further studies.

Summary

ZrO_2 and HfO_2 films, their various mixtures and two-layer nanolaminates were deposited by ALD, using $ZrCl_4$, $HfCl_4$ and H_2O. Un-doped ZrO_2 was found to be mostly in the cubic or tetragonal form, whereas un-doped HfO_2 was mostly monoclinic. Doped films exhibited the cubic zirconia structure if $Hf/(Hf+Zr) \leq 0.46$ and monoclinic hafnia if $Hf/(Hf+Zr) \geq 0.9$. Films with compositions in between aforementioned values had low peaks implying both structures or were nearly amorphous. Un-doped zirconia exhibited ferromagnetic behavior and this property diminished with the increasing amount of hafnia in the films. The highest saturation magnetization value $5 \cdot 10^{-6}$ emu and a coercivity of 50 Oe was obtained from a nanolaminate grown with 50 ALD cycles of HfO_2 and on top of it 50 ALD cycles of ZrO_2, which resulted a 10 nm HfO_2 + 8 nm ZrO_2 film and a cation ratio $Hf/(Hf+Zr) = 0.55$ and exhibited very low diffraction peaks attributable to the cubic phase. Some films exhibited both distinctive ferromagnetic characteristics and electrical polarization curves with ferroelectric component.

Acknowledgments

The present study was partially funded by the European Regional Development Fund project "Emerging orders in quantum and nanomaterials" (TK134), Spanish Ministry of Economy and Competitiveness (TEC2017-84321-C4-2-R) with support of Feder funds, Estonian Academy of Sciences (SLTFYPROF), and Estonian Research Agency (IUT2-24, PRG4).

ORCID

Kristjan Kalam https://orcid.org/0000-0001-5934-1860
Helina Seemen https://orcid.org/0000-0002-4850-0851
Raivo Stern https://orcid.org/0000-0002-6724-9834
Aile Tamm https://orcid.org/0000-0002-0547-0824
Kaupo Kukli https://orcid.org/0000-0002-5821-0364

References

1. M. F. Al-Kuhaili, "Optical properties of hafnium oxide thin films and their application in energy-efficient windows," *Optical Materials*, **27**(3), 383 (2004).
2. J. Gottmann and E. W. Kreutz, "Pulsed laser deposition of alumina and zirconia thin films on polymers and glass as optical and protective coatings," *Surface and Coatings Technology*, **116–119**, 1189 (1999).
3. M. Zukic, D. G. Torr, J. F. Spann, and M. R. Torr, "Vacuum ultraviolet thin films. 1: Optical constants of BaF_2, CaF_2, LaF_3, MgF_2, Al_2O_3, HfO_2, and SiO_2 thin films," *Appl. Opt.*, **29**, 4284 (1990).
4. S. M. Edlou, A. Smajkiewicz, and G. A. Al-Jumaily, "Optical properties and environmental stability of oxide coatings deposited by reactive sputtering," *Appl. Opt.*, **32**, 5601 (1993).
5. Y. Sorek, M. Zevin, R. Reisfeld, T. Hurvits, and S. Ruschin, "Zirconia and Zirconia−ORMOSIL Planar Waveguides Prepared at Room Temperature," *Chem. Mater.*, **9**(3), 670 (1997).
6. J. Jasieniak, J. Pacifico, R. Signorini, A. Chiasera, M. Ferrari, A. Martucci, and P. Mulvaney, "Luminescence and Amplified Stimulated Emission in CdSe–ZnS-Nanocrystal-Doped TiO_2 and ZrO_2 Waveguides," *Advanced Functional Materials*, **17**(10), 1654 (2007).
7. A. J. Waldorf, J. A. Dobrowolski, B. T. Sullivan, and L. M. Plante, "Optical coatings deposited by reactive ion plating," *Appl. Opt.*, **32**, 5583 (1993).
8. H. Obayashi, H. Okamoto, and T. Kudo, "Carbon monoxide gas sensor made of stabilized zirconia," *Solid State Ionics*, **1**(3–4), 319 (1980).
9. N. Miura, M. Nakatou, and S. Zhuiykov, "Impedancemetric gas sensor based on zirconia solid electrolyte and oxide sensing electrode for detecting total NO_x at high temperature," *Sensors and Actuators B: Chemical*, **93**(1–3), 221 (2003).
10. S. Capone, G. Leo, R. Rella, P. Siciliano, and L. Vasanelli, "Physical characterization of hafnium oxide thin films and their application as gas sensing devices," *Journal of Vacuum Science & Technology A: Vacuum, Surfaces, and Films*, **16**, 3564 (1998).
11. B. H. Lee, L. Kang, R. Nieh, W. J. Qi, and J. C. Lee, "Thermal stability and electrical characteristics of ultrathin hafnium oxide gate dielectric reoxidized with rapid thermal annealing," *Appl. Phys. Lett.*, **76**, 1926 (2000).
12. D. Wang, Q. Wang, A. Javey, R. Tu, and H. Dai, "Germanium nanowire field-effect transistors with SiO_2 and high-κ HfO_2 gate dielectrics," *Appl. Phys. Lett.*, **83**, 2432 (2003).
13. M. Houssa, V. V. Afanasiev, A. Stesmans, and M. M. Heyns, "Variation in the fixed charge density of SiO_x/ZrO_2 gate dielectric stacks during postdeposition oxidation," *Appl. Phys. Lett.*, **77**(12), 1885 (2000).
14. C-Y. Lin, S-Y. Wang, D-Y. Lee, and T-Y. Tseng, "Electrical properties and fatigue behaviors of ZrO_2 resistive switching thin films," *Journal of The Electrochemical Society*, **155**(8), H615 (2008).
15. Y. Wang, Q. Liu, S. Long, W. Wang, Q. Wang, M. Zhang, S. Zhang, Y. Li, Q. Zuo, J. Yang, and M. Liu, "Investigation of resistive switching in Cu-doped HfO_2 thin film for multilevel non-volatile memory applications," *Nanotechnology*, **21**(4), 045202 (2009).

16. S. Yu, B. Gao, H. Dai, B. Sun, L. Liu, X. Liu, R. Han, J. Kang, and B. Yu, "Improved uniformity of resistive switching behaviors in HfO_2 thin films with embedded Al layers," *Electrochemical and Solid-State Letters*, **13**(2), H36 (2010).
17. H. Y. Lee, P. S. Chen, T. Y. Wu, Y. S. Chen, C. C. Wang, P. J. Tzeng, C. H. Lin, F. Chen, C. H. Lien, and M-J. Tsai, Low power and high speed bipolar switching with a thin reactive Ti buffer layer in robust HfO_2 based RRAM, In Electron Devices Meeting, 2008. IEDM 2008. IEEE International, 1–4. IEEE, 2008.
18. T. S. Böscke, J. Müller, D. Bräuhaus, U. Schröder, and U. Böttger, "Ferroelectricity in hafnium oxide thin films," *Applied Physics Letters*, **99**(10), 102903 (2011).
19. J. Müller, T. S. Böscke, U. Schröder, S. Mueller, D. Bräuhaus, U. Böttger, L. Frey, and T. Mikolajick, "Ferroelectricity in Simple Binary ZrO_2 and HfO_2," *Nano Letters*, **12**(8), 4318 (2012).
20. S. L. Weeks, A. Pal, V. K. Narasimhan, K. A. Littau, and T. Chiang, "Engineering of Ferroelectric HfO_2-ZrO_2 Nanolaminates," *ACS Appl. Mater. Interfaces*, **9**(15), 13440 (2017).
21. X. Jia, W. Yang, M. Qin, and J. Li, "Structure and magnetism in Mn-doped zirconia: Density-functional theory studies," *Journal of Magnetism and Magnetic Materials*, **321**(15), 2354 (2009).
22. N. H. Hong, M. B. Kanoun, S. Goumri-Said, J-H. Song, E. Chikoidze, Y. Dumont, A. Ruyter, and M. Kurisu, "The origin of magnetism in transition metal-doped ZrO_2 thin films: experiment and theory," *Journal of Physics: Condensed Matter*, **25**(43), 436003 (2013).
23. J. M. D. Coey, M. Venkatesan, P. Stamenov, C. B. Fitzgerald, and L. S. Dorneles, "Magnetism in hafnium dioxide," *Physical Review B*, **72**(2), 024450 (2005).
24. P. Gao, L. J. Meng, M. P. Dos Santos, V. Teixeira, and M. Andritschky, "Characterisation of ZrO_2 films prepared by rf reactive sputtering at different O_2 concentrations in the sputtering gases," *Vacuum*, **56**(2), 143 (2000).
25. F. L. Martínez, M. Toledano-Luque, J. J. Gandía, J. Cárabe, W. Bohne, J. Röhrich, E. Strub, and I. Mártil, "Optical properties and structure of HfO_2 thin films grown by high pressure reactive sputtering," *Journal of Physics D: Applied Physics*, **40**(17), 5256 (2007).
26. H. Ikeda, S. Goto, K. Honda, M. Sakashita, A. Sakai, S. Zaima, and Y. Yasuda, "Structural and electrical characteristics of HfO_2 films fabricated by pulsed laser deposition," *Japanese journal of applied physics*, **41**(4S), 2476 (2002).
27. Y. Shen, S. Shao, H. Yu, Z. Fan, H. He, and J. Shao, "Influences of oxygen partial pressure on structure and related properties of ZrO_2 thin films prepared by electron beam evaporation deposition," *Applied surface science*, **254**(2), 552 (2007).
28. Y. Wang, Z. Lin, X. Cheng, H. Xiao, F. Zhang, and S. Zou., "Study of HfO_2 thin films prepared by electron beam evaporation," *Applied surface science*, **228**(1–4), 93 (2004).
29. M. Balog, M. Schieber, M. Michman, and S. Patai, "Chemical vapor deposition and characterization of HfO_2 films from organo-hafnium compounds," *Thin Solid Films*, **41**(3), 247 (1977).
30. T. S. Jeon, J. M. White, and D. L. Kwong, "Thermal stability of ultrathin ZrO_2 films prepared by chemical vapor deposition on Si (100)," *Applied Physics Letters*, **78**(3), 368 (2001).
31. A. Avila-García and M. García-Hipólito, "Characterization of gas sensing HfO_2 coatings synthesized by spray pyrolysis technique," *Sensors and Actuators B: Chemical*, **133**(1), 302 (2008).
32. D. Perednis, O. Wilhelm, S. E. Pratsinis, and L. J. Gauckler, "Morphology and deposition of thin yttria-stabilized zirconia films using spray pyrolysis," *Thin Solid Films*, **474**(1–2), 84 (2005).
33. K. Kukli, T. Pilvi, M. Ritala, T. Sajavaara, J. Lu, and M. Leskelä, "Atomic layer deposition of hafnium dioxide thin films from hafnium tetrakis (dimethylamide) and water," *Thin Solid Films*, **491**(1–2), 328 (2005).
34. K. Kukli, M. Ritala, J. Lu, A. Hårsta, and M. Leskelä, "Properties of HfO_2 Thin Films Grown by ALD from Hafnium tetrakis (ethylmethylamide) and water," *Journal of The Electrochemical Society*, **151**(8), F189 (2004).
35. Y-C. Lin, F. McGuire, and A. D. Franklin, "Realizing ferroelectric $Hf_{0.5}Zr_{0.5}O_2$ with elemental capping layers, Journal of Vacuum Science & Technology B," *Nanotechnology and Microelectronics: Materials, Processing, Measurement, and Phenomena*, **36**(1), 011204 (2018).
36. E. P. Gusev, C. Cabral Jr, M. Copel, C. D'emic, and M. Gribelyuk, "Ultrathin HfO_2 films grown on silicon by atomic layer deposition for advanced gate dielectrics applications," *Microelectronic Engineering*, **69**(2–4), 145 (2003).
37. H. Kim, P. C. McIntyre, and K. C. Saraswat, "Microstructural evolution of ZrO_2–HfO_2 nanolaminate structures grown by atomic layer deposition," *Journal of materials research*, **19**(2), 643 (2004).
38. K. Kukli, M. Ritala, T. Sajavaara, J. Keinonen, and M. Leskelä, "Comparison of hafnium oxide films grown by atomic layer deposition from iodide and chloride precursors," *Thin Solid Films*, **416**(1–2), 72 (2002).
39. J. Aarik, A. Aidla, A. Kikas, T. Käämbre, R. Rammula, P. Ritslaid, T. Uustare, and V. Sammelselg, "Effects of precursors on nucleation in atomic layer deposition of HfO_2," *Applied surface science*, **230**(1–4), 292 (2004).
40. K. Kukli, J. Niinistö, A. Tamm, J. Lu, M. Ritala, M. Leskelä, and M. Putkonen, "Atomic layer deposition of ZrO_2 and HfO_2 on deep trenched and planar silicon," *Microelectronic Engineering*, **84**(9–10), 2010 (2007).
41. L. Aarik, H. Alles, A. Aidla, T. Kahro, K. Kukli, J. Niinistö, and H. Mändar, "Influence of process parameters on atomic layer deposition of ZrO_2 thin films from $CpZr(NMe_2)_3$ and H_2O," *Thin Solid Films*, **565**, 37 (2014).
42. A. Tamm, J. Kozlova, L. Aarik, A. Aidla, J. Lu, A-A. Kiisler, A. Kasikov, P. Ritslaid, H. Mändar, L. Hultman, V. Sammelselg, K. Kukli, and J. Aarik, "Atomic layer deposition of ZrO_2 for graphene-based multilayer structures: In situ and ex situ characterization of growth process," *physica status solidi (a)*, **211**,(2), 397 (2014).
43. T. Arroval, L. Aarik, R. Rammula, V. Kruusla, and J. Aarik, "Effect of substrate-enhanced and inhibited growth on atomic layer deposition and properties of aluminum–titanium oxide films," *Thin Solid Films*, **600**, 119 (2016).
44. K. Kalam, H. Seemen, P. Ritslaid, M. Rähn, A. Tamm, K. Kukli, A. Kasikov, J. Link, R. Stern, S. Dueñas, and H. Castán, "Atomic layer deposition and properties of ZrO_2/Fe_2O_3 thin films," *Beilstein Journal of Nanotechnology*, **9**(1), 119 (2018).
45. J. Aarik, A. Aidla, A-A. Kiisler, T. Uustare, and V. Sammelselg, "Influence of substrate temperature on atomic layer growth and properties of HfO_2 thin films," *Thin Solid Films*, **340**(1–2), 110 (1999).
46. J. Aarik, A. Aidla, H. Mändar, T. Uustare, and V. Sammelselg, "Growth kinetics and structure formation of ZrO_2 thin films in chloride-based atomic layer deposition process," *Thin Solid Films*, **408**(1–2), 97 (2002).